

Establishing isostructural metal substitution in metalloproteins using ^1H NMR, circular dichroism, and Fourier transform infrared spectroscopy

DEAN L. POUNTNEY,¹ COLIN J. HENEHAN, AND MILAN VAŠÁK

Biochemistry Institute, University of Zürich, 8057 Zürich, Switzerland

(RECEIVED January 4, 1995; ACCEPTED June 5, 1995)

Abstract

Far-UV CD, ^1H -NMR, and Fourier transform infrared (FTIR) spectroscopy are three of the most commonly used methods for the determination of protein secondary structure composition. These methods are compared and evaluated as a means of establishing isostructural metal substitution in metalloproteins, using the crystallographically defined rubredoxin from *Desulfovibrio gigas* and its well-characterized cadmium derivative as a model system. It is concluded that analysis of the FTIR spectrum of the protein amide I resonance represents the most facile and generally applicable method of determining whether the overall structure of a metalloprotein has been altered upon metal reconstitution. This technique requires relatively little biological material (ca. 300 μg total protein) and, unlike either CD or ^1H -NMR spectroscopy, is unaffected by the presence of different metal ions, thus allowing the direct comparison of FTIR spectra before and after metal substitution.

Keywords: amide I band; far-UV CD; FTIR; isostructural metal replacement; metal substitution; NMR; rubredoxin; secondary structure

In order to study the structure of a metalloprotein, it is often necessary to replace the native metal ion, for example Zn, by another metal, such as Co, ^{113}Cd , or ^{57}Fe , the properties of which enable the structure of the protein to be probed using a certain spectroscopic technique, such as UV-visible absorption, NMR, Mössbauer, etc. The methods used to investigate metal-binding sites in proteins have been reviewed recently (Coleman, 1993; Maret & Vallee, 1993; Münck et al., 1993). Although structural alterations may occur due either to the presence of a non-native metal ion or to the preparative treatment used in obtaining a metalloderivative, the preservation of the native protein conformation in the metalloderivative is usually just assumed. The objective of the present work is to establish a suitable and facile spectroscopic method for confirming experimentally that the polypeptide fold of a metalloprotein is preserved following metal substitution. We have evaluated the suitability of three established methods for examining the secondary structure compositions of proteins that use CD, Fourier transform infrared (FTIR), and ^1H NMR spectroscopic techniques, respectively, for comparing the structures of a native and metal-substituted

metalloprotein. For this purpose, the crystallographically defined rubredoxin from *Desulfovibrio gigas* (FeRd) (Frey et al., 1987) and its well-characterized cadmium derivative (CdRd) (Henehan et al., 1993) were used as a model system.

Results

A number of analytical techniques have been reported that aim to predict the secondary structure composition of proteins based on spectroscopic properties of the peptide backbone that vary in α -helix, β -strand, and random coil conformations. The most commonly applied of these methods make use of: (1) the CD of the protein amide $n-\pi^*$ and $\pi-\pi^*$ transitions occurring in the far-UV spectral region (Provencher & Glöckner, 1981; Compton & Johnson, 1986; Yang et al., 1986; Dousseau & Pézolet, 1990; Perczel et al., 1991); (2) the principal infrared carbonyl stretching resonance of the protein amide group (Lee et al., 1990; Sarver & Krueger, 1991); or (3) the chemical shift tendencies of peptide amide protons found in ^1H NMR spectra of proteins (Wishart et al., 1991).

^1H -NMR

The chemical shift positions of the proton resonances in proteins between 8.20 and 9.0 and between 4.85 and 5.90 ppm are strongly influenced by the principal types of secondary struc-

Reprint requests to: Milan Vašák, Biochemistry Institute, University of Zürich, Winterthurerstrasse 190, 8057 Zürich, Switzerland; e-mail: mvasak@bioc.unizh.ch.

¹ Present address: Department of Biochemistry, University of Adelaide, Adelaide, South Australia 5005, Australia.

ture present (Wishart et al., 1991, and references therein). Recently, this observation has been employed in the development of simple one- and two-dimensional (2D) ^1H NMR methods for estimating the α -helix, β -strand, and random coil secondary structure contents of proteins. The utilization of these methods requires that the amino acid composition of the protein is known. For smaller proteins, where well-resolved cross-peaks in ^1H - ^1H correlated spectroscopy (COSY) spectra are usually observed, the use of this 2D NMR method is preferable. In this case, the secondary structure content of the protein is calculated using simple formulae (Equations 1–3), which rely on cross-peak counting within defined regions of the COSY spectrum obtained in H_2O (Wishart et al., 1991). Thus, for a protein containing R amino acid residues, of which G are glycine:

$$\alpha\text{-Helix (\%)} = 100[2(A - 2G)/S], \quad (1)$$

$$\beta\text{-Structure (\%)} = 100\{2[B - 0.05(R - 60)]/S\}, \quad (2)$$

$$\text{Random coil (\%)} = 100[(0.9C)/S], \quad (3)$$

where A , B , and C are the numbers of peaks counted in areas a, b, and c in Figure 1, and S is the overall sum of the numerators in each of the three equations (Wishart et al., 1991).

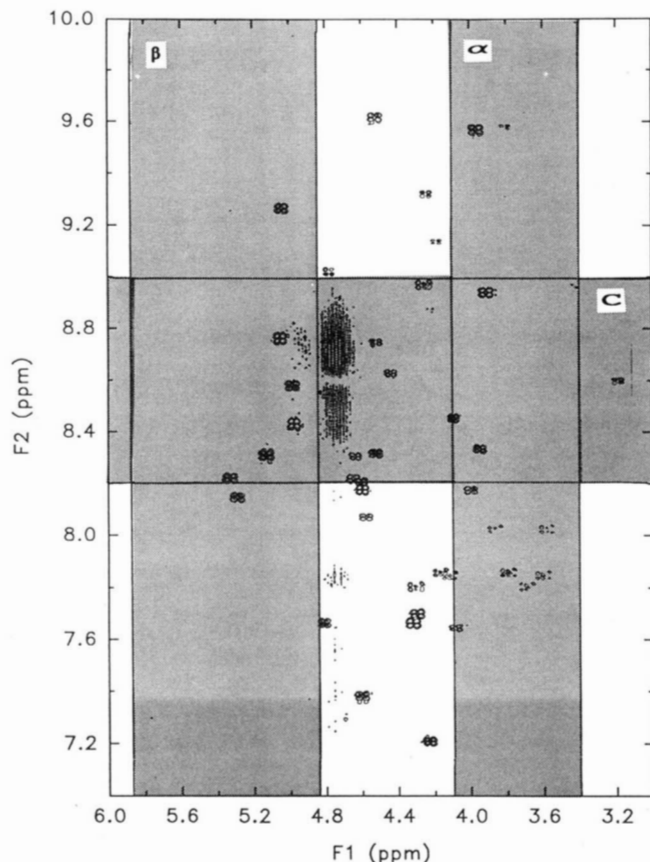


Fig. 1. Fingerprint region of the ^{113}Cd -decoupled DQF-COSY ^1H NMR spectrum of CdRd at 300 K, showing peak counting regions (see text for details).

The ^{113}Cd -decoupled double quantum-filtered (DQF)-COSY ^1H NMR spectrum of $^{113}\text{CdRd}$ is characterized by a number of well-resolved cross-peaks in the “fingerprint” region between 7.0 and 10.0 ppm in the F2 dimension and between 3.0 and 6.0 ppm in the F1 dimension (Fig. 1). Application of Equations 1–3 yields 6% α -helix, 45% β -structure, and 49% random coil (see Table 1). However, due to the presence of a paramagnetic Fe(III) center in the native FeRd, proton resonances close to this metal center are broadened and/or isotropically shifted (data not shown), effects that do not permit meaningful secondary structure analysis to be performed.

Far-UV CD

Regular stretches of secondary structure in proteins are characterized by excitonic coupling of the principal electronic transition of adjacent peptide amide chromophores, giving rise to two transitions of different energies with oppositely signed CD (Bayley, 1980; Woody, 1985). In the case of the α -helix, for example, the amide π - π^* transition at 190 nm is split into two components at (+)190 and (–)206 nm. Quantum mechanical mixing of the negative component at 206 nm with the amide n - π^* transition leads to the appearance of a second CD feature at 222 nm with the same sign. As the excitonic coupling is dependent upon the relative orientation of the coupled transition dipole moments, each type of protein secondary structure, i.e., α -helix, β -sheet, β -turn, random coil, exhibits its own characteristic CD spectrum in the far-UV region (below 240 nm). This forms the basis for the prediction of protein secondary structure composition using CD spectroscopy. Proportions of each secondary structure type are obtained by spectral deconvolution of the protein CD spectrum as a linear sum of predetermined basis spectra. In our CD analysis, the deconvolution method of Provencher and Glöckner (1981) (CONTIN) with the selection of the estimate with five degree of freedom (Manavalan & Johnson, 1987) and the convex constraint analysis (CCA) method of Perczel et al. (1991) were used. The former method analyzes for α -helix, β -sheet, and remainder based on a data set of CD spectra of proteins with known X-ray structure. Because the Provencher and Glöckner method does not analyze for β -turn, the CCA method was also applied. The latter method derives

Table 1. Comparison of predicted secondary structure compositions (%) of native (FeRd) and cadmium-substituted (CdRd) rubredoxin from *D. gigas* with the X-ray structure of the native protein (Frey et al., 1987)

	Helix		β		Random coil
	α	3_{10}	Turns	Sheet	
X-ray	8	12	9	21	50
NMR ^a	6	[-----45-----]			49
CD ^b (CCA)	0	[-----43-----]		0	57
CD ^b (CONTIN)	10	[-----34-----]			56
FTIR ^c	[-----28-----]		15	17	40

^a CdRd only.

^b FeRd only.

^c Both CdRd and FeRd yielded identical analytical results.

the spectral contributions of each of the secondary structure elements directly from the experimental CD curves of a set of globular proteins. The individual component CD spectra obtained by deconvolution of the CD spectra of the set of proteins are then assigned based on their correspondence to the known CD profiles of individual secondary structure types (Perczel et al., 1991, 1992; Perczel & Fasman, 1992). The only variable that must be determined for each analysis is the number of pure component CD curves, P , represented in the data set. In our CCA analysis, the data set of 23 proteins supplied with the program has been used. Regarding the correlation coefficients between the calculated and X-ray structures for the total set of individual secondary structure elements, we refer to the work of Perczel et al. (1992).

The CD spectrum of native FeRd (Fe(III)) exhibits two negative extrema at 201 nm and 225 nm and a positive extremum at 192 nm (Fig. 2). The analysis of this CD profile using the method of Provencher and Glöckner as described above resulted in $10 \pm 1\%$ α -helix, $34 \pm 2\%$ β -sheet, and $56 \pm 2\%$ remainder (Table 1). With the CCA method the most satisfactory analysis of the basis set of CD spectra, including that of FeRd, was obtained using five pure component curves ($P = 5$), three of which could readily be identified as α -helix, β -sheet, and random coil, respectively, and the remaining two were classified as additional chiral contributions, perhaps originating from other unusual types of secondary structure, disulfides, or higher energy π - π^* transitions of aromatic amino acids (Bolotina & Lugauskas, 1985) (data not shown). The determined pure component curves were used in the subsequent analysis of the CD spectrum of FeRd. The best fit was obtained using only two of the template curves, one of which is assigned as random coil (57%), the other as an additional chiral contribution (43%) (Fig. 2; Table 1). Although the latter chiral component curve does not correspond to any of the pure component curves reported for known secondary structure types, it best approximates a type of β -turn structure (Perczel & Fasman, 1992a). Note that according to the crystal structure, rubredoxin *D. gigas* contains no ordinary α -helix, but has four "helical corners," composed of three amino acid residues each, in which the first turn is identical with the 3_{10} -helix and the second with the hair-

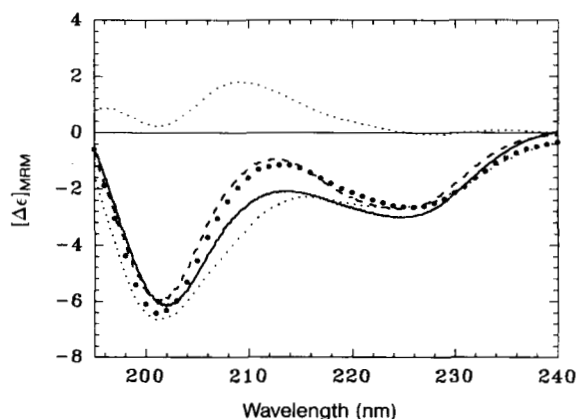


Fig. 2. Far UV-CD spectra of FeRd (dashed line) and CdRd (solid line), illustrating the composite spectra of FeRd (thin dotted lines) and overall fit (fat dotted line) obtained by convex constraint analysis (see text for details).

pin type I bend structure (Frey et al., 1987). Thus, the results of both CD analyses with about 44% of the ordered secondary structure and 56% random coil structure are very similar.

The CD spectrum of the CdRd derivative is significantly altered compared to that of the native protein (Fig. 2), primarily due to a filling of the trough between the two major negative bands and the superposition of a weak derivative-shaped feature between 225 and 255 nm. In our previous 2D NMR and optical studies of CdRd, these differences have been assigned to chiral contributions of the optically active CysS-Cd(II) LMCT transitions of the $(\text{Cd}(\text{CysS})_4)^{2-}$ center (Henehan et al., 1993). A similar conclusion has also been reached in the CD studies of the Cd-substituted GAL4 protein (Pan & Coleman, 1990). Moreover, the absence of analogous transitions in FeRd in the spectral region used for the secondary structure analysis has been demonstrated (Henehan et al., 1993). Consequently, the changes observed in the CD spectrum of CdRd cannot be taken as evidence for a change in the protein fold upon metal substitution and hence no analysis of this spectrum has been attempted. However, the high-energy region (below 200 nm) of the CD spectrum, which has a substantially higher content of secondary structure information (Compton & Johnson, 1986), is outside the range of CysS-Cd(II) LMCT chromophores and may be used for the comparison of the protein fold. This region of the CD spectrum is identical in both rubredoxin metalloderivatives.

FTIR

IR spectra of proteins and polypeptides are characterized by a number of so-called amide bands that represent different vibrations of the peptide moiety, each representing the combined but variable contributions of the peptide C=O, C-N, and N-H bonds. The major factors responsible for conformational sensitivity of amide bands include hydrogen bonding and coupling between transition dipoles (Surewicz et al., 1993). The amide I band is the most widely used for secondary structure determination. This vibrational mode originates almost entirely from the amide carbonyl stretching vibration of the peptide bond, which produces one or more intense peaks in the $1,600$ – $1,700\text{-cm}^{-1}$ region of the IR spectrum, depending on the geometrical arrangements of peptide groups. The individual overlapping components represent the contributions from the IR spectra of α -helical, β -sheet, β -turn, and random coil regions of the protein. Therefore, deconvolution of the absorption envelope using multivariate statistical procedures and a spectral database of proteins of known spatial structure (see Fig. 3) can yield an estimate of secondary structure composition.

The FTIR spectra of FeRd and CdRd in H_2O are closely similar (Fig. 4), each exhibiting an absorption maximum at $1,653\text{ cm}^{-1}$, a distinct shoulder at $\sim 1,620\text{ cm}^{-1}$, and a slight shoulder at $\sim 1,668\text{ cm}^{-1}$. The spectra were analyzed using the multicomponent analysis software PLS Quant (Mattson) and the reference data set of proteins with known secondary structure content illustrated in Figure 3. Consistent with the insensitivity of this method to bound metal ions, the analyses of both metalloderivatives of Rd are identical (Table 1).

Discussion

The present study allows a number of conclusions concerning the establishment of isostructural metal substitution in proteins

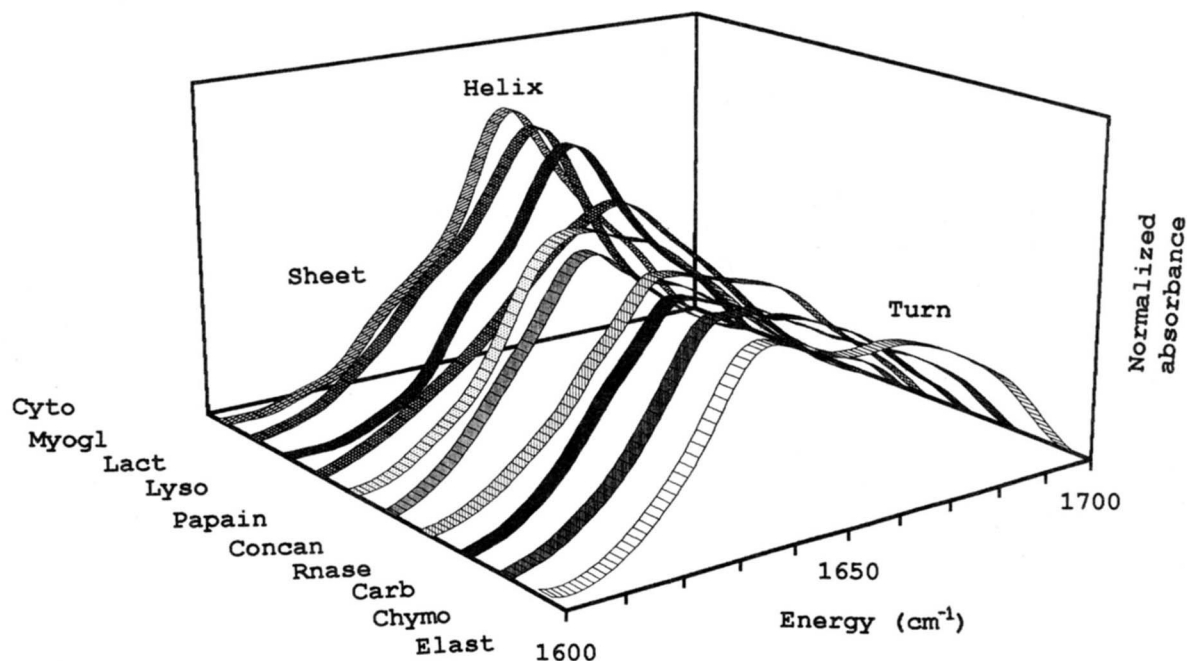


Fig. 3. FTIR spectra of 10 standard proteins in the region of the amide I transition, indicating helix, sheet, and turn regions (see text for experimental details and abbreviations).

to be drawn. The suitability of far-UV CD, FTIR, and $^1\text{H-NMR}$ techniques as methods for comparing metalloprotein structure before and after metal reconstitution have been assessed using FeRd and CdRd as a model system. We have established in previous studies that these two rubredoxin metalloforms have identical three-dimensional structures (Henehan et al., 1993). A comparison of the secondary structure content of both Rd metalloderivatives, obtained using the various predictive methods, with that of X-ray data is summarized in Table 1. The results of the secondary structure analyses generally correspond quite well with the X-ray crystal structure data (Table 1), with the NMR method showing the greatest overall accuracy. The relative merits of the predictive techniques for establishing isostructural metal substitution in metalloproteins and their sensitivities

are summarized in Table 2. Of these methods, the NMR method offers the highest degree of resolution, however, it is not in general appropriate for paramagnetic systems and is limited to small proteins (<20 kDa) (Wishart et al., 1991) (see Table 2).

Although highly sensitive, the use of the CD method is clearly not appropriate for systems containing metal ions, such as Cd(II) and Zn(II), which often exhibit optically active LMCT absorptions in the spectral region of interest, i.e., 180–260 nm. In particular, the presence of intense CD features between 250 and 210 nm for the CysS-Cd(II) chromophore and between 235 and 200 nm for the CysS-Zn(II) chromophore are well documented (Vašák & Kägi, 1983; Henehan et al., 1993). The influence of such optically active chromophores on the CD analysis will be much less significant in larger proteins. Thus, in Rd *D. gigas* (52 amino acids), the contribution of CysS-Cd(II) LMCT bands to the CD intensity of the protein at 212 nm is 50% of the total intensity. Whereas, in the case of a large pro-

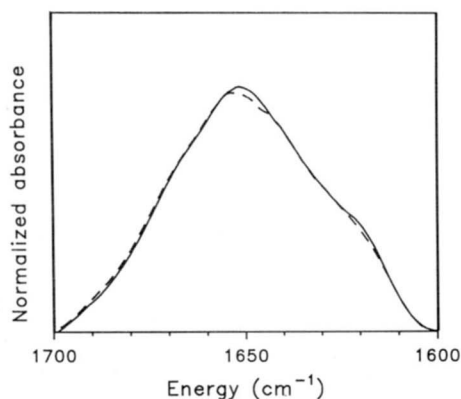


Fig. 4. FTIR spectra of FeRd (solid line) and CdRd (dashed line) in the region of the amide I transition (see text for details).

Table 2. Relative merits of techniques for establishing isostructural metal substitution in metalloproteins

	Predictive accuracy	Sensitivity	Comments
NMR	Good	1 μmol	Cannot be used for proteins >20 kDa or in the presence of paramagnetic metal ions
CD	Fair	1–2 nmol	Subject to interference from LMCT bands
FTIR	Fair	100 μg	No interferences; direct spectral comparison possible

tein, such as the dimeric enzyme liver alcohol dehydrogenase, which contains two zinc centers per subunit (374 amino acids) with two and four cysteine ligands, respectively, much less of the total intensity of the CD signals will be due to the LMCT chromophores. The far-UV CD spectrum of this metalloprotein (native and Cd-substituted forms) is dominated by the CD features of the polypeptide backbone (Drum & Vallee, 1970).

The ability of FTIR spectroscopy to detect small changes in protein structure introduced, for instance, by site-directed mutagenesis (Haris & Chapman, 1992; Bowler et al., 1993), by Ca(II) binding to the apoforms of Ca(II)-binding proteins (Jackson et al., 1991), etc., has been demonstrated. Moreover, using the vibrational bands of metal-coordinating COO⁻ groups in parvalbumin, differences in coordination of Ca(II)-, Mg(II)-, and Mn(II)-bound forms have been shown (Nara et al., 1994). The FTIR analyses of both FeRd and CdRd are closely similar and fit reasonably well with the crystal structure of the protein (see Table 1). Clearly, the amide I region is not affected by the nature of the bound metal ion making direct spectral comparison before and after metal substitution possible. Thus, FTIR is the method of choice for establishing isostructural metal replacement in metalloproteins (see Table 2).

Materials and methods

Rubredoxin from *D. gigas* (FeRd) was obtained from Dr. M. Bruschi, Marseille. The cadmium derivative (CdRd) was prepared as described previously (Henehan et al., 1993). The following proteins were obtained from either Fluka, Boehringer, or Sigma, and used for the FTIR database without further purification: bovine pancreas α -chymotrypsin A (Chymo), *Canavalia ensiformis* concanavalin A (Concan), horse heart cytochrome *c* type VI (Cyto), hog pancreas elastase (Elast), rabbit muscle L-lactate dehydrogenase (Lact), muramidase lysozyme (Lyso), sperm whale skeletal muscle myoglobin (Myogl), *Carica papaya* papain (papain), bovine pancreas ribonuclease (Rnase), bovine erythrocyte carbonic anhydrase (Carb).

DQF-COSY ¹H NMR spectra were recorded at 27 °C on a Bruker AMX-600 spectrometer using standard pulse sequences. The NMR sample (2 mM protein in 50 mM [²H₁₁]Tris-HCl, 0.1 M NaCl, pH 7.6) in 10% D₂O/90% H₂O was measured in a 5-mm NMR tube. Chemical shift positions are reported relative to the 4.80-ppm resonance of H₂O.

CD spectra were measured on a Jasco 500-C spectropolarimeter interfaced with a microcomputer, using a time constant of 16 s, a 2-nm spectral bandwidth, and a scan speed of 1 nm min⁻¹. The spectral region from 200 to 183 nm was averaged over four scans in order to improve the signal-to-noise ratio. The protein concentration was 3.35 × 10⁻⁵ M in 50 mM potassium phosphate, pH 7.0, with a cell pathlength of 0.02 cm. A buffer spectrum was recorded under the same experimental conditions as the sample and subtracted. The protein concentration was calculated using the extinction coefficient of RdDg, $\epsilon_{278} = 17,210$ M⁻¹ cm⁻¹ (Moura et al., 1991), from the absorption spectrum of a concentrated stock solution. CD spectra were analyzed using the program CCA obtained from Dr. A. Perczel and the program CONTIN obtained from Dr. S.W. Provencher.

FTIR spectra were recorded using a Philips PU9624 FTIR spectrometer and analyzed with a modification of the procedure of Lee et al. (1990) using the multicomponent analysis program PLS Quant (Philips). Five hundred twelve scans were averaged,

apodized with a Happ-Genzler function, and Fourier transformed to give a resolution of better than 2 cm⁻¹. Demountable calcium fluoride cells (Buck Scientific) were used with a 15- μ m teflon spacer. The sample (ca. 10 μ L) was introduced using a 20- μ L Gilson pipette inserted firmly into the filling hole of the assembled cell. Using a 15- μ m spacer, as opposed to the 6- μ m spacer more commonly used for protein FTIR spectral measurements, markedly improved the pathlength reproducibility (see Lee et al., 1990). The temperature of the cell was maintained at a constant 21 ± 0.5 °C throughout the measurement. A sample shuttle was used to interleave background and sample spectra. Buffer spectra were recorded in the same cells and under the same instrument conditions as the sample spectra. All proteins for FTIR measurement were dialyzed against 50 mM potassium phosphate buffer, pH 7.0, and subsequently concentrated to 10–30 mg/mL in an ultrafiltration apparatus (Amicon). The buffer spectrum was subtracted from the protein spectrum using an interactive subtraction routine (95–99%). A proper subtraction of water was judged to yield an approximately flat baseline from 1,900 to 1,700 cm⁻¹, avoiding negative side lobes, and removal of the water band near 2,130 cm⁻¹. The spectrum was subsequently smoothed using a 13-point Savitzky-Golay smoothing function. Spectra were then corrected by extrapolating a linear baseline from 1,600 to 1,700 cm⁻¹ and normalizing the ordinate to zero. Finally, the curves were divided by their integrals in order to normalize the spectra to a constant area and multiplied by 100 for convenience.

The conformational percentages of FeRd and the model proteins (see above) were obtained from X-ray crystallographic data using the definition of Kabsch and Sander (1983). The γ -turns, which are [*i*, *i* + 2] hydrogen bonded, are included in the total β -turns, and α - and π -helices, which are [*i*, *i* + 4] and [*i*, *i* + 5] hydrogen bonded, respectively, are put into the α -helix category. Similarly, parallel and antiparallel β -pleated sheets are both put into the β -sheet category. The percentages of the various hydrogen bonded categories were called from the DSSP (define secondary structure of protein) file of the ProteinData directory on the netserver at EMBL, Heidelberg, electronic mail address: netserv@embl-heidelberg.de.

Acknowledgments

We gratefully acknowledge Prof. J.H.R. Kägi for helpful discussions and Dr. O. Zerbe for measuring the ¹H NMR spectra. This work was supported by the Swiss National Science Foundation grant 31-32572.91.

References

- Bayley P. 1980. Circular dichroism and optical rotation. In: Brown SB, ed. *An introduction to spectroscopy*. London: Academic Press. pp 148–190.
- Bolotina IA, Lugauskas VY. 1985. Determination of the secondary structure of proteins from the circular dichroism spectra. Consideration of the contribution of aromatic amino acid residues to the circular dichroism spectra of proteins in the peptide region. *J Mol Biol* 190:1154–1166.
- Bowler EB, May K, Zaragoza T, York P, Dong A, Caughey WS. 1993. Destabilization effects of replacing a surface lysine of cytochrome *c* with aromatic amino acids: Implication for the denaturated state. *Biochemistry* 32:183–190.
- Coleman JE. 1993. Cadmium-113 nuclear magnetic resonance applied to metalloproteins. *Methods Enzymol* 227:16–43.
- Compton LA, Johnson WC Jr. 1986. Analysis of protein circular dichroism spectra for secondary structure using a simple matrix multiplication. *Anal Biochem* 155:155–167.
- Dousseau F, Pérolet M. 1990. Determination of the secondary structure con-

- tent of proteins in aqueous solutions from their amide I and amide II infrared bands. Comparison between classical and partial least-squares methods. *Biochemistry* 29:8771-8779.
- Drum DE, Vallee BL. 1970. Optical properties of catalytically active cobalt and cadmium liver alcohol dehydrogenases. *Biochem Biophys Res Commun* 41:33-39.
- Frey M, Sieker L, Payan F, Haser R, Bruschi M, Pep G, LeGall J. 1987. Rubredoxin from *Desulfovibrio gigas*: A molecular model of the oxidised form at 1.4 Å resolution. *J Mol Biol* 197:525-541.
- Haris PI, Chapman D. 1992. Does Fourier-transform infrared spectroscopy provide useful information on protein structures? *Trends Biochem Sci* 17:328-333.
- Henehan CJ, Pountney DL, Zerbe O, Vašák M. 1993. Identification of cysteine ligands in metalloproteins using optical and NMR spectroscopy: Cadmium-substituted rubredoxin as a model $[\text{Cd}(\text{Cys})_4]^{2-}$ center. *Protein Sci* 2:1756-1764.
- Jackson M, Haris PI, Chapman D. 1991. Fourier transform infrared spectroscopic studies of Ca^{2+} -binding proteins. *Biochemistry* 30:9681-9686.
- Kabsch W, Sander C. 1983. Dictionary of protein secondary structure: Pattern recognition of hydrogen-bonded and geometrical features. *Biopolymers* 22:2577-2637.
- Lee DC, Harris PI, Chapman K, Mitchell UC. 1990. Determination of protein secondary structure using factor analysis of infrared spectra. *J Am Chem Soc* 29:9185-9193.
- Manavalan P, Johnson WC Jr. 1987. Variable selection method improves the prediction of protein secondary structures from circular dichroism spectra. *Anal Biochem* 167:76-87.
- Maret W, Vallee BL. 1993. Cobalt as probe and label of proteins. *Methods Enzymol* 226:52-71.
- Moura I, Teixeira M, LeGall J, Moura JJJ. 1991. Spectroscopic studies of cobalt and nickel substituted rubredoxin and desulforedoxin. *J Inorg Biochem* 44:127-139.
- Münck E, Suberus KK, Hendrich MP. 1993. Combining Mössbauer spectroscopy with integer spin electron paramagnetic resonance. *Methods Enzymol* 226:463-479.
- Nara M, Tasumi M, Tanokura M, Hiraoiki T, Yazawa M, Tsutsumi A. 1994. Infrared studies of interaction of metal ions with Ca^{2+} -binding proteins. Marker bands for identifying the types of coordination of side-chain COO^- groups to metal ions in pike parvalbumin ($\text{pI} = 4.10$). *FEBS Lett* 349:84-88.
- Pan T, Coleman JE. 1990. The DNA binding domain of GAL4 forms a binuclear metal ion complex. *Biochemistry* 29:3023-3029.
- Perczel A, Fasman GD. 1992. Quantitative analysis of cyclic β -turn models. *Protein Sci* 1:378-395.
- Perczel A, Hollosi M, Tusnady G, Fasman GD. 1991. Convex constraint analysis: A natural deconvolution of circular dichroism curves of proteins. *Protein Eng* 4:669-679.
- Perczel A, Park K, Fasman GD. 1992. Deconvolution of the circular dichroism spectra of the proteins: The circular dichroism spectra of antiparallel β -sheet. *Proteins Struct Funct Genet* 13:57-69.
- Provencher SW, Glöckner J. 1981. Estimation of globular protein secondary structure from circular dichroism. *Biochemistry* 20:33-37.
- Sarver RW Jr, Krueger WC. 1991. Protein secondary structure from Fourier transform infrared spectroscopy: A data base analysis. *Anal Biochem* 194:89-100.
- Surewicz WK, Mantsch HH, Chapman D. 1993. Determination of protein secondary structure by Fourier transform infrared spectroscopy: A critical assessment. *Biochemistry* 32:389-394.
- Vašák M, Kägi JHR. 1983. Spectroscopic properties of metallothionein. *Metal Ions Biol Systems* 15:213-273.
- Wishart DS, Sykes BD, Richards FM. 1991. Simple techniques for the quantification of protein secondary structure by ^1H NMR spectroscopy. *FEBS Lett* 293:72-80.
- Woody RW. 1985. Circular dichroism of peptides. *Peptides* 7:15-113.
- Yang JT, Wu CSC, Martinez HM. 1986. Calculation of protein conformation from circular dichroism. *Methods Enzymol* 130:208-269.